JOURNAL OF AGRICULTURAL AND FOOD CHEMISTRY
ARTICLE

J. Agric. Food Chem. 2009, 57, 7005–7012 7005
DOI:10.1021/jf9010164

Autoclave and β-Amylolysis Lead to Reduced in Vitro Digestibility of Starch

B. Elliot Hickman, Srinivas Janaswamy, and Yuan Yao*

Whistler Center for Carbohydrate Research and Department of Food Science, Food Science Building, Purdue University, West Lafayette, Indiana 47907-1160

In this study, a combination of autoclave and β-amylolysis was used to modulate the digestibility of normal corn starch (NCS) and wheat starch (WS). The modification procedure comprised three cycles of autoclave at 35% moisture content and 121 °C, β-amylolysis, and one additional cycle of autoclave. Starch materials were sampled at each stage and characterized. The fine structure of starch was determined using high-performance size-exclusion chromatography, the micromorphology of starch dispersion was imaged using cryo-SEM, the crystalline pattern was evaluated using wide-angle X-ray powder diffraction, and the digestibility was measured using Englyst assay. After β-amylolysis, amylose was enriched (from 25.4 to 33.2% for NCS and from 27.5 to 32.8% for WS) and the branch density was increased (from 5.2 to 7.7% for NCS and from 5.3 to 7.9% for WS). Cryo-SEM images showed that the autoclave treatment led to the formation of a low-swelling, high-density gel network, whereas β-amylolysis nearly demolished the network structure. The loss of A-type crystalline structure and the formation of B- and V-type structures resulted from autoclave, which suggests the formation of amylose-based ordered structure. Englyst assay indicated that, due to β-amylolysis, the resistant starch (RS) content was increased to 30 from 11% of native NCS and to 23 from 9% of native WS. In contrast, autoclave showed only minor impact on RS levels. The increase of RS observed in this study is associated with enhanced branch density, which is different from the four types of RS commonly defined.

KEYWORDS: Starch; autoclave; β-amylolysis; digestibility

INTRODUCTION

Starch is a primary carbohydrate polymer of higher plants and constitutes a major source of carbohydrate intake in the human diet. In past decades, substantial efforts have been made to manipulate the digestibility of starch, and an increase in the level of resistant starch has been the goal most often pursued. Resistant starch is understood as the starch elements that escape hydrolysis in the small intestine and thus are available for colon fermentation. According to Englyst et al. (*1*), by its susceptibility to amylolytic enzymes, starch can be classified into rapidly digestible starch (RDS), slowly digestible starch (SDS), and resistant starch (RS). In addition, RS can be classified into RS type 1 (physically inaccessible starch), RS type 2 (granular starch), RS type 3 (retrograded starch), and RS type 4 (chemically modified starch). The strategy to produce different types of RS has been extensively discussed (*2*).

Linear α-glucans such as amylose or debranched amylopectin, and starch materials rich in linear glucans, are favored for preparing RS. High-amylose maize starch (HAMS), which usually contains > 50% of amylose, is the most preferred material for producing RS-containing food ingredients (*2*). Starches with regular or low amylose content have also been used to prepare RS and SDS after enzymatic debranching (*3*−*5*). Debranching releases linear chains from amylopectin; thus, the retrogradation can be improved. A limitation of RS prepared from debranched non-HAMS is related to the presence of very short chains, which are not likely to form double helices and crystallite (*6*). Eerlingen et al. (*7*) indicated that the chain length of RS ranges from DP19 to DP26 and is independent of the chain length of amylose and that chains shorter than DP24 are unlikely to be involved in crystallization.

Hydrothermal treatments have been used to improve the RS level. For example, the chain mobility of HAMS can be enhanced by acid treatment, thus improving the rearrangement of chains during annealing and heat−moisture treatment (*8*). Among hydrothermal treatments, autoclave has been used to improve RS content (*9*−*17*). It was indicated that autoclave-mediated formation of RS can be affected by the amylose content (*10*), treatment time and the presence of acid (*16*), the use of lintnerization (*15*), and plant genotypes (*14*). Interestingly, it was also reported that the RS amount obtained using high-pressure autoclave was similar to the values obtained after gelatinization in a boiling water bath (*12*).

Another approach to reduce the digestibility of starch material is to increase the content of α-1,6 linkages, that is, to increase the branch density (*18*−*20*). The reduction of digestibility is due to the lower susceptibility of α-1,6 linkages to amyloglucosidase than α-1,4 linkages (*21*, *22*). Our previous work showed that highly branched malto-oligosaccharides and a

*Corresponding author [telephone (765) 494-6317; fax (765) 494-7953; e-mail yao1@purdue.edu].

Published on Web 07/02/2009

highly branched α-glucan, phytoglycogen, offer lower digestibility (*20*) than normal and waxy corn starch. Usually, the preparation of these materials requires substantial starch degradations and conversion or needs to utilize certain maize mutants.

In this study, our goal is to establish a new strategy which incorporates amylose retrogradation and enhanced amylopectin branch density for the preparation of starch materials with reduced digestibility. Normal corn starch and wheat starch were used as model systems due to their low cost and suitability for hydrothermal and enzymatic modifications. In this study, we hypothesize that the dextrins after β-amylolysis of starch have a much reduced digestibility compared with native starches and starches subjected to autoclave. In the meantime, we attempted to achieve the β-amylolysis in a relatively high solid content (20%), which would be beneficial for potential industrial applications.

MATERIALS AND METHODS

Materials. Normal corn starch and high-amylose corn starch (HylonVII) were obtained from National Starch and Chemical Co. (Bridgewater, NJ). Wheat starch was obtained from MGP Ingredients Inc. (Manhattan, KS). Pancreatin and amyloglucosidase were purchased from Sigma. Isoamylase, pullulanase, and GOPOD assay kit were purchased from Megazyme (Ireland). β-Amylase (BBA) was a gift from Genencor (Rochester, NY). The activity of β-amylase was 16400 Betamyl units/mL determined using the Betamyl method (Megazyme).

β-Amylolysis of Autoclaved Starches. The moisture contents of normal corn starch (NCS) and wheat starch (WS) were adjusted to 35% using deionized water. The starch was pressed through a 20 mesh sieve to form a collection of loosely compacted grains. The grains were then subjected to three cycles of autoclave of 30 min each at 121 °C with a 15 min temperature ramp-up and a 15 min ramp-down for each thermal cycle. Immediately after cooling, the material was dried to <10% moisture content in a fluid bed dryer (Stability Products, Rochelle, IL) at 45 °C. The material was dry-ground to pass through an 80 mesh sieve (180 μm). The starch powders thus obtained were termed NCS-AT (AT = autoclave) for NCS-based and WS-AT for WS-based.

Portions of starch materials NCS-AT and WS-AT were suspended in pH 5.5, 0.02 M NaAc buffer to form 20% (dry base) suspension. β-Amylase was added to this solution at a dose of 0.5% based on dry starch. The reaction was delivered in a shaking water bath at 55 °C at 70 rpm for 20 h. Then the reactants were centrifuged at 3000*g* for 10 min, and the supernatant and starch precipitate were collected. The supernatant was immediately heated in a boiling water bath for 10 min to terminate the action of β-amylase. To denature β-amylase and remove the maltose mixed in the starch precipitate, three weights of ethanol were added, dispersed, and filtered. This was followed by an additional five times of dispersion−filtration washing of starch residue using 80% ethanol. Finally, ethanol was added to dehydrate starch, which was followed by a complete evaporation of ethanol in a fume hood. The starch solid was ground and passed through an 80 mesh sieve to obtain NCS-AT-BA and WS-AT-BA (BA = β-amylolysis).

Portions of powder material NCS-AT-BA and WS-AT-BA were adjusted to a moisture content of 35% using deionized water. Thereafter, the material was pressed through a 20 mesh sieve and treated by one cycle of autoclave with the thermal conditions described above. The dry powder was obtained using a fluid bed dryer, ground, and passed through an 80 mesh sieve. These materials were termed NCS-AT-BA-AT and WS-AT-BA-AT. The names of samples were given according to the sequential treatments they received. For example, NCS-AT-BA-AT indicates a NCS-based material receiving sequentially autoclave, β-amylolysis, and autoclave. To evaluate the maltose retained in starch material, the dispersion−filtration procedure using 50% ethanol was conducted for NCS-AT-BA, WS-AT-BA, NCS-AT-BA-AT, and WS-AT-BA-AT followed by dehydration. HPSEC analysis of debranched starch materials showed a negligible amount of residual maltose.

HPSEC Analysis of Starch Chain Length Distribution. To determine the chain length distribution of starch after enzymatic modification, high-performance size exclusion chromatography (HPSEC) was used. Five milligrams of starch material was dispersed in 125 μL of 90% DMSO and heated in a boiling water bath for 10 min. Sodium acetate buffer (0.02 M, 875 μL, 50 °C, pH 4.75) was added to dispersion. The mixture was heated again in a boiling water bath for 10 min and cooled to 37 °C in a shaking water bath. Isoamylase solution (Megazyme, 5 U/mL, 50 μL in acetate buffer) was added to each mixture. The mixtures were incubated for 24 h at 37 °C with constant agitation and then boiled for 10 min. The samples were cooled, and pullulanase solution (Megazyme, 7.2 U/mL, 40 μL in acetate buffer) was added to each sample. The mixtures were incubated for another 24 h at 37 °C and then boiled for 10 min. Moisture was removed using a centrifugal vacuum concentrator (SpeedVac, Savant). The volume of each sample was adjusted to 1 mL with 90% DMSO. After vortex and centrifugation to remove insolubles, a 20 μL aliquot was injected into the HPSEC system. The HPSEC system contains two connected Zorbax gel PSM 60-S columns (6.2 × 250 mm, Agilent Technologies, Santa Clara, CA) and a flow rate of 0.5 mL/min with DMSO as the mobile phase. The elution was monitored by a Waters 2414 refractive index (RI) detector (Waters, Milford, MA). Glucose, maltose, maltotriose, maltotetraose, and pullulan with molecular weights of 5900, 11800, 22800, 47300, 112000, and 212000, respectively (Polymer Laboratories, Amherst, MA), were used for column calibration. For each starch, HPSEC data processing includes raw data exportation to an Excel spreadsheet and normalization of the chromatogram by the total area from retention time of 10−20 min.

For each sample, amylose content was determined from the chromatogram by integrating the area from the 10 min point to the lowest point at the right side of the first peak (amylose peak). To determine the branch density, the chromatogram (mass-based) was converted to that of molar-based using a calibration curve (*23*). The average chain length (average CL) was determined by the following equation: average $CL = \Sigma(NM)/\Sigma N$. For starch without β-amylolysis (NCS, WS, NCS-AT, WS-AT), the integration region was from 10 to 17.5 min to include the entire area of debranched starch. For starch after β-amylolysis, due to the presence of small sugars such as maltose after debranching, the integration region was conducted from 10 to 19 min to include the entire area of debranched starch. The branch density was determined as the inverse of CL.

Cryo-SEM Imaging. In a 2 mL centrifuge tube, 50 mg of starch material (dry basis) was mixed with deionized water to form 1.0 mL of a 5% starch suspension. The suspension was vortexed and heated in a boiling water bath for 10 min. Repetitive vortexing was conducted during the heating. After cooling, the starch dispersion was immediately delivered for cryo-SEM imaging. At the cryo-SEM facility, the dispersion was deposited into a specimen stub and frozen in liquid nitrogen slush. The sample was transferred to the Gatan Alto 2500 prechamber cooled to about −170 °C. There, the sample was fractured with a scalpel to produce a free-break surface followed by sublimation. The sublimation was conducted for 30 min at −80 °C followed by platinum coating. Then the sample was transferred to the microscope cryo-stage and imaged with an FEI NOVA nanoSEM field emission SEM using the TLD (through-the-lens) or ET (Everhart−Thornley) detector operating at 5 kV accelerating voltage, approximate 4.0−5 mm working distance, spot 2.7−3, and aperture 6.

In Vitro Digestibility Using the Englyst Assay. The in vitro digestibility of starch was measured according to the protocol described by Englyst et al. (*1*) with modifications. All starch suspensions containing added guar gum were heated in a boiling water bath for 10 min. After cooling and stabilization in a 37 °C water bath, the enzyme preparation was added. The enzyme preparation contains pancreatin and amyloglucosidase prepared according to the Englyst assay protocol (*1*). During the digestion, the reactant was aliquoted at 20, 40, 60, 90, and 120 min and mixed with 2 volumes of anhydrous ethanol. The mixtures were used as the stock solutions for glucose assay. The GOPOD procedure was conducted using an assay kit (Megazyme). Glucose yield at 0 min was considered to be zero, because HPSEC analysis showed that the glucose in each starch sample was negligible.

DSC Analysis. To evaluate the ordered structure of native and modified starch, differential scanning calorimetry (DSC) was used and

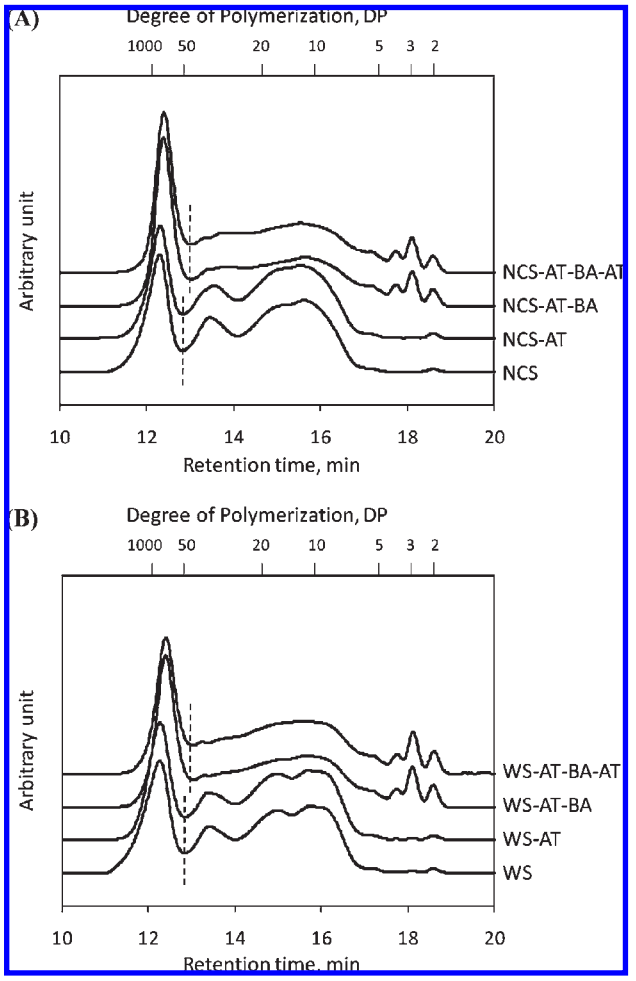

Figure 1. Chain length distribution of normal corn starch (**A**) and wheat starch (**B**) subjected to autoclave and β-amylolysis. The vertical dashed lines indicate the borders used to differentiate the linear chains released from amylose (left) and amylopectin (right).

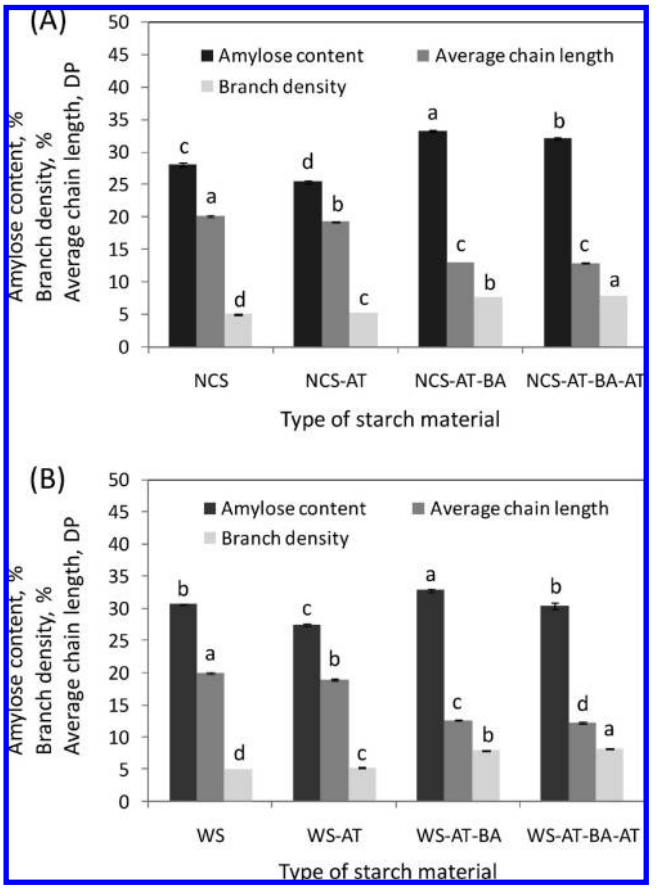

Figure 2. Amylose content, average chain length, and branch density of individual starch materials. Data are expressed as mean with error bar of standard deviation ($n = 3$). Significant differences within each category are denoted by different letters ($p < 0.05$).

calibrated using indium. The DSC unit used was a TA standard modulated DSC 2920. For each sample starch tested, 5 mg (dry weight) was added to a standard TA hermetic aluminum pan, and then deionized water was added, bringing the total sample weight to 16.6 mg and making a 30% solid dispersion. The pan was sealed and allowed to equilibrate for 2 h at room temperature before being loaded into the DSC unit. DSC for each sample was performed beginning with equilibration at 30 °C, held isothermal for 3 min. The temperature within the DSC unit cell was then raised at 5 °C/min to 140 °C. Data were collected and evaluated by Universal Analysis software. Due to the pressure limitation for aluminum pans, it would be difficult to identify the amylose-related endothermic peak above 100 °C. However, this analysis allowed us to evaluate the organized structure formed primarily by amylopectin.

X-ray Powder Diffraction. About 500 mg of starch sample was packed into an aluminum holder and mounted on a Philips PW3710 diffractometer interfaced to a personal computer equipped with Automated Powder Diffraction (APD) software. Ni-filtered Cu Kα radiation ($\lambda = 1.5418$ Å) was used, and the tube was operated at 40 kV and 25 mA. The intensity data were collected at room temperature at 0.01° intervals in the 2θ range from 10° to 38°, and the time spent at each step was 4 s. The patterns were smoothed for further analysis by the PC-APD (version 3.6) software, and such a process resulted in 695 data points for the entire pattern.

The crystallinity of starch was determined as described in a previous paper (*24*). Initially around 450 data points in the nonpeak regions were selected as background points and a ninth-order polynomial was fitted using Origion 7.5 Evaluation version (http://www.originlab.com) for generating the background profile. Background intensity at each measured diffraction angle (2θ) was estimated using cubic spline interpolation methodology. The percentage of crystallinity was calculated as follows:

$$\%\text{crystallinity} = (\text{total area} - \text{background profile area}) \times 100/\text{total area}$$

RESULTS AND DISCUSSION

Impact of Autoclave and β-Amylolysis on Starch Fine Structure. **Figure 1** shows the fine structure of native normal corn starch (NCS) and wheat starch (WS) and their derivatives subjected to autoclave and β-amylolysis. For both NCS- and WS-based groups, the impact of autoclave on the amount and molecular weight of amylose appears to be minor. As shown in **Figure 2**, for NCS-based materials the amylose content was reduced from 28.0% for NCS to 25.4% for NCS-AT and from 33.2% for NCS-AT-BA to 32.0% for NCS-AT-BA-AT. For WS-based materials, the amylose was reduced from 30.6% for WS to 27.5% for WS-AT and from 32.8% for WS-AT-BA to 30.4% for WS-AT-BA-AT. By comparing the chromatograms between NCS and NCS-AT (**Figure 1A**) and between WS and WS-AT (**Figure 1B**), it appears that the reduction of amylose amount after autoclave was accompanied by a slight reduction of the high molecular weight component of amylose.

The observation of a reduction of amylose content has not been reported. However, it is reasonable to assume that a hash hydrothermal treatment such as repetitive autoclaves may result in minor degradation of amylose. We further consider that the high molecular weight portion of amylose could be more

susceptible to hydrothermal degradation, which is reflected by a reduction of this portion in HPSEC chromatograms. Such a reduction may lead to the production of a minor amount of a short linear segment. In the HPSEC analysis of debranched starch, these amylose-originated short linear chains may elute with the chains of debranched amylopectin. This may result in a reduced amylose content determined using molecular weight distribution in chromatograms.

The impact of autoclave on amylopectin chain length distribution was negligible for NCS, WS, and their derivatives as determined by HPSEC analysis. It appears that even though a number of short linear chains can be released from amylose and incorporated in the amylopectin population in the chromatograms, the overall HPSEC profile for the amylopectin region (**Figure 1**) was not appreciably affected by autoclave.

The impact of β-amylolysis on starch fine structure was profound. The chromatogram comparison (**Figure 1**) between NCS-AT and NCS-AT-BA and between WS-AT and WS-AT-BA shows that the molecular weight of amylose and chain length distribution of amylopectin were substantially affected by β-amylolysis. By comparing the chromatograms between NCS-AT and NCS-AT-BA (**Figure 1A**) and between WS-AT and WS-AT-BA (**Figure 1B**), it is evident that β-amylolysis shifted the amylose peaks to the low molecular weight region, demonstrating a substantial shortening of linear chains. For amylopectin, β-amylolysis created a number of maltosyl, maltotriosyl, and maltotetraosyl stubs. Due to the presence of maltotetraosyl stubs, it can be concluded that the β-amylolysis did not reach the limit. For NCS, the limit of β-amylolysis, that is, the upper limit of maltose yield, is around 55% (*25*). In our study, the reducing sugar analysis showed maltose yields of 46.6 and 48.3% for NCS and WS, respectively.

The impacts of β-amylolysis on amylose content, average chain length, and branch density of starch materials are shown in **Figure 2**. For the NCS-based materials, β-amylolysis increased the amount of amylose population from 25.4% (NCS-AT) to 33.2% (NCS-AT-BA). For the WS-based materials, the amylose population was increased from 27.5% (WS-AT) to 32.8% (WS-AT-BA). We consider that the amylose enrichment by β-amylolysis was basically caused by a preferential hydrolysis of β-amylase on amylopectin molecules due to their much more abundant nonreducing ends compared with amylose.

β-Amylolysis reduces the average chain length (CL) by trimming maltosyl units sequentially from the nonreducing end of glucan external chains. For NCS-based materials, the average CL was reduced from 19.2 DP (DP = degree of polymerization) for NCS-AT to 13.0 DP for NCS-AT-BA (**Figure 2**). For WS-based materials, the average CL was reduced from 19.0 DP for WS-AT to 12.6 DP for WS-AT-BA. The branch density calculated as the reverse of average CL is also shown in **Figure 2**. After β-amylolysis, the branch density increased from 5.2 to 7.7% for NCS-based materials and from 5.3 to 7.9% for WS-based materials.

Impact of Autoclave and β-Amylolysis on the Micromorphology of Starch Dispersion. Figure 3 shows the cryo-SEM images of 5% dispersions of NCS, NCS-AT, NCS-AT-BA, and NCS-AT-BA-AT. For NCS, the discontinuous phase contains meshes smaller than those in the continuous phase. We would consider that the discontinuous phase comprises swollen starch granules or their disrupted pieces. In contrast, the continuous phase contains leached materials, such as amylose. For NCS-AT, the heterogeneity of dispersion is also evident. Starch particles formed by grinding were dispersed in a continuous phase. The gel networks inside these particles are extremely dense compared with that of NCS, suggesting the role of autoclave in forming junction zones that are resistant to swelling.

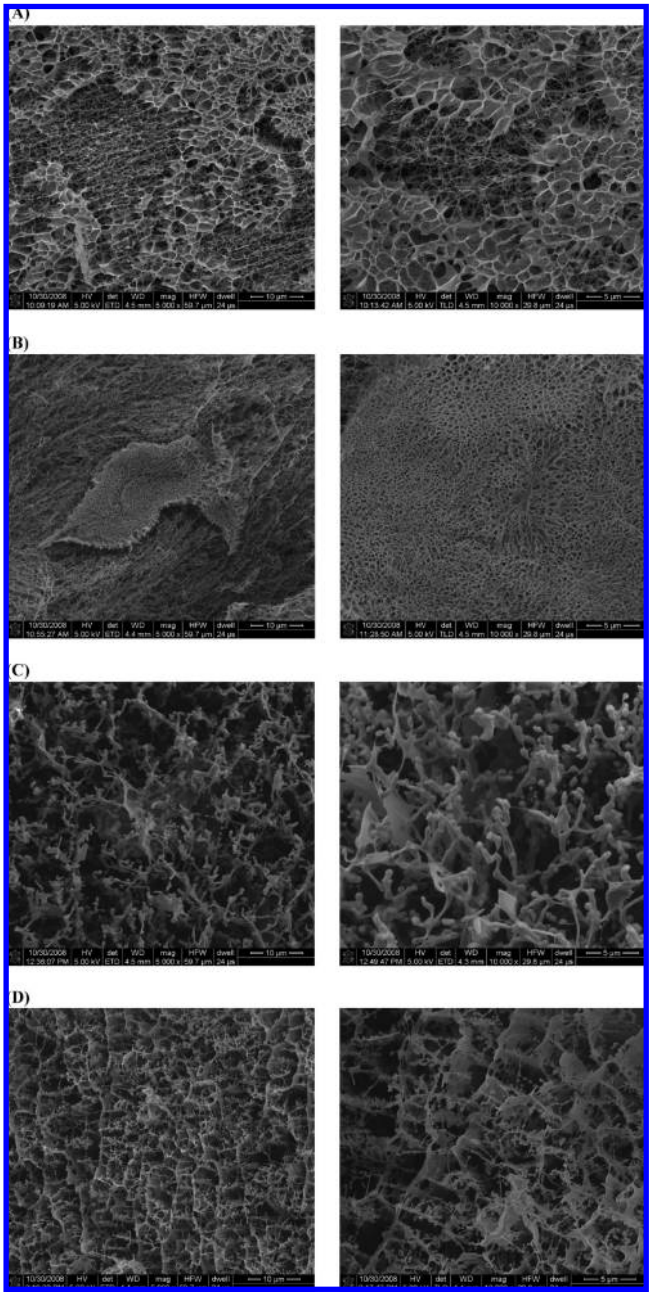

Figure 3. Cryo-SEM images of NCS (**A**), NCS-AT (**B**), NCS-AT-BA (**C**), and NCS-AT-BA-AT (**D**).

The application of β-amylolysis completely changed the micromorphology of the starch dispersion, resulting in a noncohesive pattern (**Figure 3C**). As shown for NCS-AT-BA, β-amylolysis removed the capability of starch residues to form appreciable networks in a time scale of approximately 10 min (needed to deliver samples) after 100 °C treatment. It is interesting that autoclave may change the micromorphology of starch treated with β-amylase. For NCS-AT-BA-AT, a wall-like continuous connection was formed among individual hollow segments (**Figure 3D**).

It was not a surprise that β-amylolysis substantially reduced the potential of starch to form gel network. β-Amylase trims off external chains of both amylopectin and amylose. This action leads to the exposure of branches with short stubs, which may cause steric hindrance to the interactions among individual glucan molecules. On the other hand, autoclave may have enforced the formation of junction zones among the trimmed

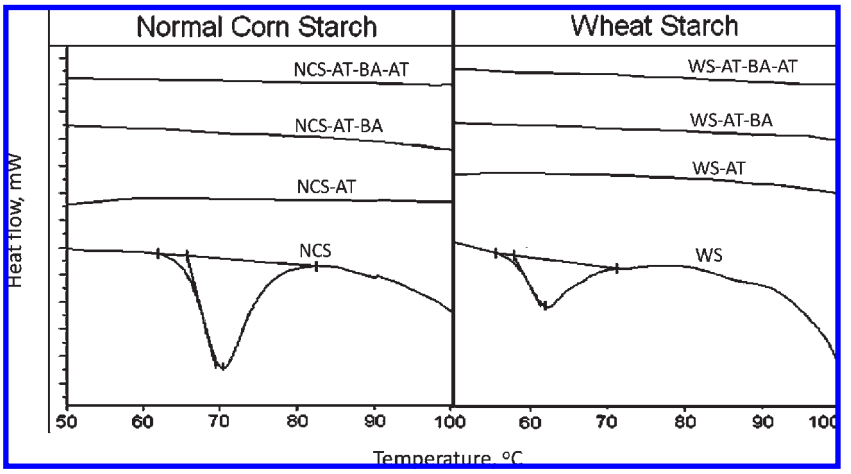

Figure 4. DSC profiles of individual starch samples.

segments, which was observed from the images of NCS-AT-BA-AT. Particularly, the autoclave might facilitate interactions among amylose residues.

DSC Profiles of Treated Starch Materials. As shown by **Figure 4**, the endothermic peaks below 100 °C were negligible for all treated starches compared with their native counterparts. This indicates a complete removal of amylopectin ordered structure due to the three-cycle autoclave at 35% moisture content. In contrast, our previous work (*24*) showed that NCS and WS samples heated to 95 °C at 40% moisture content retain a significant amount of amylopectin ordered structure. Apparently, the much higher temperature (121 °C) applied in the autoclave resulted in a complete removal of amylopectin ordered structure at the moisture content of 35%, and no amylopectin retrogradation occurred during the dehydration of autoclaved samples and the β-amylolysis treatment. On the other hand, amylose retrogradation may occur during the repetitive autoclave treatment. Due to the pressure limitation for hermetic aluminum pans, the amylose-related endothermic peak (at higher temperature range) was not detected. Therefore, we used X-ray powder diffraction to evaluate the organization of amylose.

X-ray Powder Diffraction of Starch Materials. The diffraction patterns of NCS and WS and their treated samples are shown in **Figure 5**. In general, the patterns are indicative of the semicrystalline nature of the sample. In the case of native NCS and WS the diffraction pattern is mainly composed of six characteristic profiles observed at 11.2°, 15.0°, 16.8°, 18.0°, 20.0°, and 23.1° of 2θ. These reflections are indicative of A-type starch diffraction (*26*). The crystallinities for NCS and WS are 16.4 and 13.2%, respectively.

Autoclave and β-amylolysis have pronounced effects on the overall diffraction pattern. First, the A-type pattern was almost completely lost due to the autoclave treatment, suggesting the transformation of ordered amylopectin chain organization to an amorphous state. This is consistent with the DSC evaluation. Second, two new peaks around 13.0° and 20.0° are observed, suggesting the V-starch formation (*27*, *28*). In addition, the two well-resolved profiles observed at 16.8° and 18.0° in both native starches got merged, which demonstrates the formation of B-type starch (*26*). These major changes of crystalline diffraction pattern indicate the impact of autoclave on the organization of amylose and amylopectin. In other words, autoclave removes amylopectin-based ordered structure and generates amylose-based ordered structure. It is interesting to note that β-amylolysis after autoclave did not lead to a fundamental change in the overall pattern that contains both V- and B-type starch diffraction.

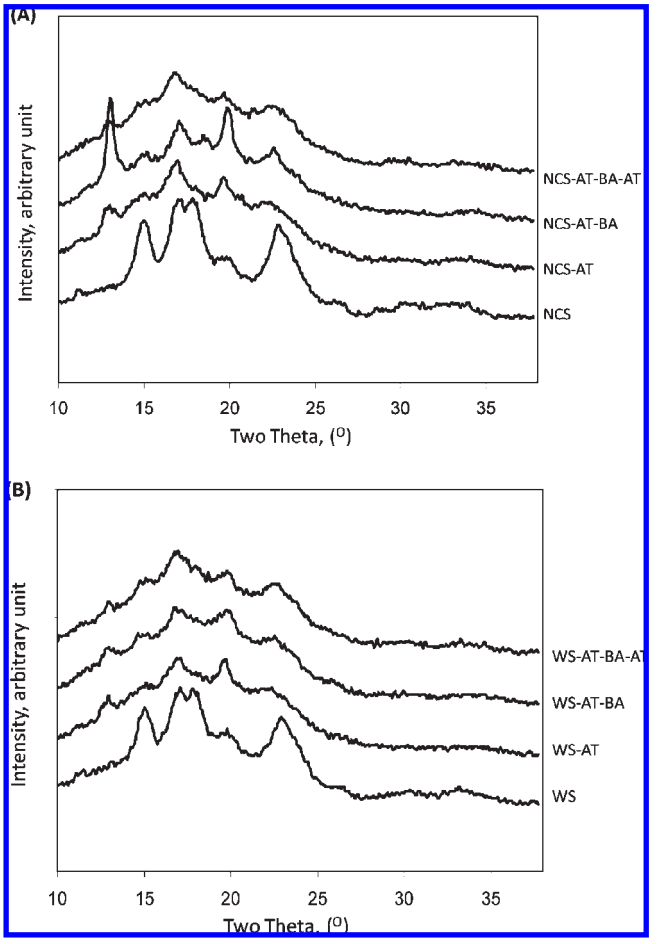

Figure 5. X-ray powder diffraction patterns of treated normal corn starch (**A**) and wheat starch (**B**) compared with their native counterparts.

The pattern of NCS-AT-BA was somewhat abnormal, in which the 13.0° and 20.0° peak intensities of V-type starch were much higher than those of the other treated samples. However, after one cycle of autoclave (NCS-AT-BA-AT), the peak intensities at both 13.0° and 20.0° were reduced to the level of NCS-AT. The crystallinity indices for these three samples were 8.8, 10.2, and 8.2, respectively. The presence of a greater amount of V-starch in NCS-AT-BA seems to be responsible for its increased crystallinity. Similar type of V- and B-type diffraction is also seen for treated WS group samples, however, with a little lower

crystallinity values, 7.2, 7.2 and 7.9, in the same order of the treatment. It is interesting to note that, for the WS-based materials, the abnormal high V-starch peaks were not observed for WS-AT-BA, although it underwent the same procedure as NCS-AT-BA. Whereas the reason for such high intense V-type peaks with NCS-AT-BA was not identified in this study, we consider that the starch dehydration using ethanol could be a factor. Perhaps both ethanol treatment and starch origin contribute to such a behavior.

***β*-Amylolysis Is the Governing Factor of Reduced Starch Digestibility. Figure 6** shows the Englyst digestibility profile of treated starches as compared with their native starches and high-amylose starch (Hylon VII). The Englyst assay was used due to its correlation with human study (*1*) for the reference to actual digestion performances. Overall, all starch materials after *β*-amylolysis showed a much reduced digestibility compared with native starches and starches with autoclave only. For NCS-based materials, the digestibility of NCS-AT-BA and NCS-AT-BA-AT approaches that of high-amylose starch, the primary starting material for producing RS. In contrast, the digestibility of WS-based starch materials WS-AT-BA and WS-AT-BA-AT ranges between that of native WS and high-amylose starch. The RS contents of starch materials are listed in **Table 1**. As references, the RS contents of NCS, WS, and HylonVII were 11.4, 9.1, and 35.4%, respectively. Three cycles of autoclave moderately increase RS content to 13.3 and 10.9% for NCS- and WS-based groups, respectively. It appears that autoclave led to substantial change of crystalline pattern but not an appreciable reduction of digestibility. In contrast, *β*-amylolysis increases the RS contents to 29.9 and 23.1% for NCS- and WS-based groups, respectively. As expected, an additional cycle of autoclave had limited effect on RS content, that is, no change for the NCS group and an increase from 23.1 to 27.8% for the WS group.

In this study, the *β*-amylolysis of starch is a much more important factor than autoclave for reduced digestibility and increased RS level. **Figure 7** shows a schematic of gelatinized starch micromatrix. Here we use a "fringed micelle" model to describe starch microstructure that contains the ordered regions formed by amylose segments and the amorphous regions composed of nonassociated amylose segments, amylopectin clusters, and amylopectin intercluster chains. For starch subjected to *β*-amylolysis, amylopectin clusters contain stubs in place of chains with regular length.

All starch samples were freshly cooked before Englyst assay. For native starch and starch subjected to the three-cycle autoclave, the immediate enzyme digestion does not allow the retrogradation of amylopectin to occur. For samples subjected to *β*-amylolysis, amylopectin retrogradation is thermodynamically unfavored due to the much reduced chain length (*6*, *29*). For all starch materials studied, there are several types of region in the model: amorphous regions of amylopectin clusters including the branching zones and external chains, ordered regions of associated or crystallized amylose, and amorphous regions containing amylose and amylopectin intercluster chains. These regions have different susceptibilities to enzymes. The branching zones of amylopectin clusters may have a low susceptibility to amyloglucosidase compared with the external chains. The regions of associated or crystallized amylose may have a low accessibility to α-amylase compared with amorphous regions. In contrast,

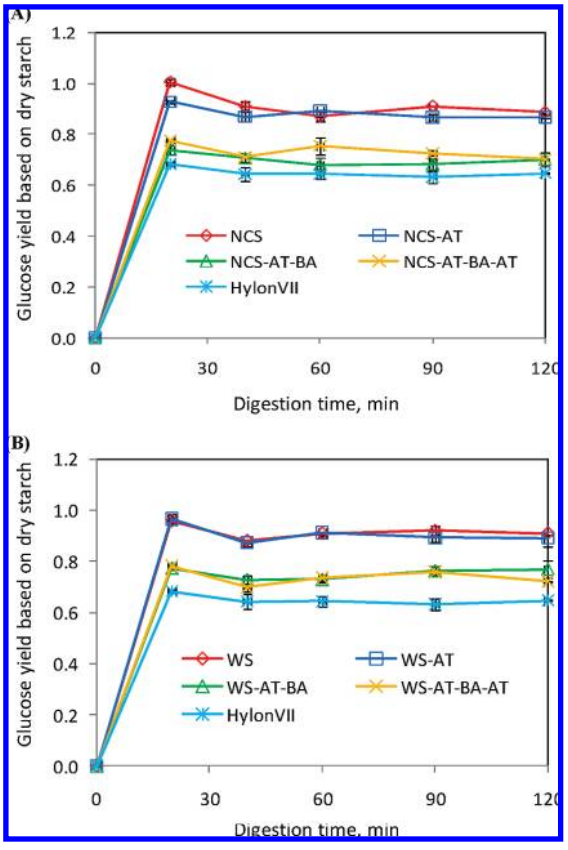

Figure 6. Englyst digestion profiles of treated normal corn starch (**A**) and wheat starch (**B**) compared with those of native starches and high-amylose starch (Hylon VII). The error bar denotes the standard deviation of four measurements.

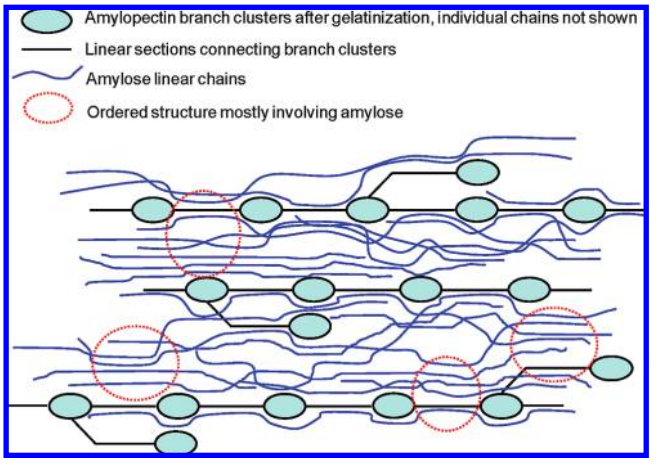

Figure 7. Schematic of fringed micelle model depicting different regions in starch.

Table 1. Resistant Starch Content (Percent) of Starch Materials after Autoclave and *β*-Amylolysis[a]

normal corn starch				wheat starch				
NCS	NCS-AT	NCS-AT-BA	NCS-AT-BA-AT	WS	WS-AT	WS-AT-BA	WS-AT-BA-AT	Hylon VII
11.4 ± 0.5	13.3 ± 0.4	29.9 ± 2.7	29.8 ± 0.2	9.1 ± 0.9	10.9 ± 1.1	23.1 ± 3.5	27.8 ± 0.2	35.4 ± 0.1

[a] Data are presented as mean±SD (n = 4).

amorphous regions containing nonassociated amylose and the amylopectin internal segments are readily susceptible to a combined action of α-amylase and amyloglucosidase. The relative abundance of these regions governs the overall digestibility of starch.

The RS content of native NCS and WS mostly originates from the branching zones of amylopectin clusters and the associated or crystallized amylose generated after the 100 °C cooking. Autoclave of native starches led to the formation of amylose-based crystallites (**Figure 5**); however, it did not increase the RS amount compared with native starches. This suggests two possibilities. First, the branching points rather than the organized amylose regions are the primary factors of RS in native starch. Second, whereas organized amylose regions may contribute to RS, autoclave did not show its advantage due to the formation of an equivalent amount of organized amylose after the 100 °C cooking procedure right before the Englyst test. This outcome possibly reflects the results of Garcia-Alonso et al. (*12*) that autoclave and boiling water bath cooking led to similar RS amounts.

The trimming of amylopectin and amylose chains due to β-amylolysis has two outcomes. First, the branching zones of amylopectin clusters were enriched, leading to an overall reduced susceptibility to amyloglucosidase. Second, the shortening of amylopectin external chains may reduce the interaction between amylose and amylopectin, which may contribute to a more efficient amylose−amylose association. Both outcomes may contribute to a significant reduction of digestibility and increased RS level.

The RS materials generated in this study are different from those conventionally defined, that is, RS type 1 for physically inaccessible starch, RS type 2 for granular starch, RS type 3 for retrograded starch, and RS type 4 for chemically modified starch. For these four types of RS, the resistance to digestion is mostly originated from their low susceptibility to α-amylase. In other words, their structural (either physical or chemical) integrity inhibits the efficient hydrolysis by α-amylase. In this study, the starch materials subjected to β-amylolysis showed an open physical structure (**Figure 3**), which excludes any barrier effect to α-amylase. Apparently, the reduced susceptibility to amyloglucosidase due to enriched branch points was the primary factor of reduced digestibility and increased RS. By efficiently improving RS of low-cost commodity starches such as normal corn starch and wheat starch, this study may have potential industrial values.

LITERATURE CITED

(1) Englyst, H.; Kingman, S.; Cummings, J. Classification and measurement of nutritionally important starch fractions. *Eur. J. Clin. Nutr.* **1992**, *46* (Suppl. 2), 33−50.

(2) Thompson, D. Strategies for the manufacture of resistant starch. *Trends Food Sci. Technol.* **2000**, *11*, 245–253.

(3) Guraya, H. S.; James, C.; Champagne, E. T. Effect of enzyme concentration and storage temperature on the formation of slowly digestible starch from cooked debranched rice starch. *Starch−Staerke* **2001**, *53*, 131–139.

(4) Guraya, H. S.; James, C.; Champagne, E. T. Effect of cooling and freezing on the digestibility of debranched rice starch and physical properties of the resulting material. *Starch−Staerke* **2001**, *53*, 64–74.

(5) Shin, S. I.; Choi, H. J.; Chung, K. M.; Hamaker, B. R.; Park, K. H.; Moon, T. W. Slowly digestible starch from debranched waxy sorghum starch: preparation and properties. *Cereal Chem.* **2004**, *81*, 404–408.

(6) Gidley, M. J.; Bulpin, P. V. Crystallization of maltooligosaccharides as models of the crystalline forms of starch—minimum chain-length requirement for the formation of double helices. *Carbohydr. Res.* **1987**, *161*, 291–300.

(7) Eerlingen, R. C.; Deceuninck, M.; Delcour, J. A. Enzyme-resistant starch. 2. Influence of amylose chain-length on resistant starch formation. *Cereal Chem.* **1993**, *70*, 345–350.

(8) Brumovsky, J. O.; Thompson, D. B. Production of boiling-stable granular resistant starch by partial acid hydrolysis and hydrothermal treatments of high-amylose maize starch. *Cereal Chem.* **2001**, *78*, 680–689.

(9) Nyman, M.; Pedersen, B.; Siljestrom, M.; Asp, N.; Eggum, B. Formation of enzyme resistant starch during autoclaving of wheat-starch: studies *in vitro* and *in vivo*. *J. Cereal Sci.* **1987**, *6*, 159–172.

(10) Escarpa, A.; Gonzalez, M. C.; Manas, E.; Garcia-Diz, L.; Saura-Calixto, F. Resistant starch formation: standardization of a high-pressure autoclave process. *J. Agric. Food Chem.* **1996**, *44*, 924–928.

(11) Skrabanja, V.; Kreft, I. Resistant starch formation following autoclaving of buckwheat (*Fagopyrum esculentum* Moench) groats. An in vitro study. *J. Agric. Food Chem.* **1998**, *46*, 2020–2023.

(12) Garcia-Alonso, A.; Jimenez-Escrig, A.; Martin-Carron, N.; Bravo, L.; Saura-Calixto, F. Assessment of some parameters involved in the gelatinization and retrogradation of starch. *Food Chem.* **1999**, *66*, 181–187.

(13) Jimenez-Escrig, A.; Martin-Carron, N.; Bravo, L.; Saura-Calixto, F. Assessment of some parameters involved in the gelatinization and retrogradation of starch. *Food Chem.* **1999**, *66*, 181–187.

(14) Skrabanja, V.; Liljeberg, H.; Hedley, C.; Kreft, I.; Bjorck, I. Influence of genotype and processing on the in vitro rate of starch hydrolysis and resistant starch formation in peas (*Pisum sativum* L.). *J. Agric. Food Chem.* **1999**, *47*, 2033–2039.

(15) Aparicio-Saguilan, A.; Flores-Huicochea, E.; Tovar, J.; Garcia-Suarez, F.; Gutierrez-Meraz, F.; Bello-Perez, L. A. Resistant starch-rich powders prepared by autoclaving of native and lintnerized banana starch: partial characterization. *Starch−Staerke* **2005**, *57*, 405–412.

(16) Onyango, C.; Bley, T.; Jacob, A.; Henle, T.; Rohm, H. Influence of incubation temperature and time on resistant starch type III formation from autoclaved and acid-hydrolysed cassava starch. *Carbohydr. Polym.* **2006**, *66*, 494–499.

(17) Gonzalez-Soto, R.; Mora-Escobedo, R.; Hernandez-Sanchez, H.; Sanchez-Rivera, M.; Bello-Perez, L. The influence of time and storage temperature on resistant starch formation from autoclaved debranched banana starch. *Food Res. Int.* **2007**, *40*, 304–310.

(18) Lee, C.; Le, Q.; Kim, Y.; Shim, J.; Lee, S.; Park, J.; Lee, K.; Song, S.; Auh, J.; Lee, S.; Park, K. Enzymatic synthesis and properties of highly branched rice starch amylose and amylopectin cluster. *J. Agric. Food Chem.* **2008**, *56*, 126–131.

(19) Ao, Z.; Simsek, S.; Zhang, G.; Venkatachalam, M.; Reuhs, B.; Hamaker, B. Starch with a slow digestion property produced by altering its chain length, branch density, and crystalline structure. *J. Agric. Food Chem.* **2007**, *55*, 4540–4547.

(20) Shin, J.; Simsek, S.; Reuhs, B.; Yao, Y. Glucose release of water-soluble starch-related α-glucans by pancreatin and amyloglucosidase is affected by the abundance of α-1,6-glucosidic linkages. *J. Agric. Food Chem.* **2008**, *56*, 10879–10886.

(21) Pazur, J.; Ando, T. The hydrolysis of glucosyl oligosaccharides with α-D-(1,4) and α-D-(1,6) bonds by fungal amyloglucosidase. *J. Biol. Chem.* **1960**, *235*, 297–302.

(22) Pazur, J.; Kleppe, K. The hydrolysis of α-D-glucosides by amyloglucosidase from *Aspergillus niger*. *J. Biol. Chem.* **1962**, *237*, 1002–1006.

(23) Yao, Y.; Thompson, D.; Guiltinan, M. Maize starch branching enzyme (SBE) isoforms and amylopectin structure: in the absence of SBEIIb, the further absence of SBEIa leads to increased branching. *Plant Physiol.* **2004**, *136*, 515–3523.

(24) Hickman, B. E.; Janaswamy, J.; Yao, Y. Properties of starch subjected to partial gelatinization and β-amylolysis. *J. Agric. Food Chem.* **2009**, *57*, 666−674.

(25) Yun, S.; Matheson, N. Structures of the amylopectins of waxy, normal, amylose-extender, and wx-ae genotypes and of the phytoglycogen of maize. *Carbohydr. Res.* **1993**, *243*, 307–321.

(26) Cairns, P.; Bogracheva, T.; Ring, S.; Hedley, C.; Morris, V. Determination of the polymorphic composition of smooth pea starch. *Carbohydr. Polym.* **1997**, *32*, 275–282.

(27) Buleon, A.; Colonna, P.; Planchot, V.; Ball, S. Starch granules: structure and biosynthesis. *Int. J. Biol. Macromol.* **1998**, *23*, 85–112.

(28) Nuessli, J.; Putaux, J.; Le Bail, P.; Buleon, A. Crystal structure of amylose complexes with small ligands. *Int. J. Biol. Macromol.* **2003**, *33*, 227–234.

(29) Yao, Y.; Zhang, J.; Ding, X. Partial β-amylolysis retards starch retrogradation in rice product. *J. Agric. Food Chem.* **2003**, *51*, 4066–4071.

Received March 27, 2009. Revised manuscript received June 16, 2009. Accepted June 17, 2009.